Developmental Biology xxx (2011) xxx–xxx

Contents lists available at ScienceDirect

Developmental Biology

journal homepage: www.elsevier.com/developmentalbiology

The transcription factor HLH-2/E/Daughterless regulates anchor cell invasion across basement membrane in *C. elegans*

Adam J. Schindler, David R. Sherwood *

Department of Biology, Duke University, Durham, NC 27708, USA

ARTICLE INFO

Article history:
Received for publication 12 February 2011
Revised 17 June 2011
Accepted 7 July 2011
Available online xxxx

Keywords:
Anchor cell
Cell invasion
Transcriptional regulation
Basement membrane
HLH-2

ABSTRACT

Cell invasion through basement membrane is a specialized cellular behavior critical for many developmental processes and leukocyte trafficking. Invasive cellular behavior is also inappropriately co-opted during cancer progression. Acquisition of an invasive phenotype is accompanied by changes in gene expression that are thought to coordinate the steps of invasion. The transcription factors responsible for these changes in gene expression, however, are largely unknown. *C. elegans* anchor cell (AC) invasion is a genetically tractable *in vivo* model of invasion through basement membrane. AC invasion requires the conserved transcription factor FOS-1A, but other transcription factors are thought to act in parallel to FOS-1A to control invasion. Here we identify the transcription factor HLH-2, the *C. elegans* ortholog of *Drosophila* Daughterless and vertebrate E proteins, as a regulator of AC invasion. Reduction of HLH-2 function by RNAi or with a hypomorphic allele causes defects in AC invasion. Genetic analysis indicates that HLH-2 has functions outside of the FOS-1A pathway. Using expression analysis, we identify three genes that are transcriptionally regulated by HLH-2: the protocadherin *cdh-3*, and two genes encoding secreted extracellular matrix proteins, *mig-6*/*papilin* and *him-4*/*hemicentin*. Further, we show that reduction of HLH-2 function causes defects in polarization of F-actin to the invasive cell membrane, a process required for the AC to generate protrusions that breach the basement membrane. This work identifies HLH-2 as a regulator of the invasive phenotype in the AC, adding to our understanding of the transcriptional networks that control cell invasion.

Introduction

Basement membranes (BMs) are dense, highly cross-linked forms of extracellular matrix that underlie all epithelia and endothelia. BMs regulate cell differentiation and polarization as well as provide structural and barrier functions (Rowe and Weiss, 2008). Despite their barrier function, BMs are regularly traversed by specialized cells during development and immune surveillance. For example, trophoblast cells breach the endometrium to establish the placenta, and leukocytes cross the perivascular BM to reach sites of infection (Madsen and Sahai, 2010; Pollheimer and Knofler, 2005). The genetic networks that control invasive behavior are also thought to be co-opted by tumor cells during metastasis (Gertler and Condeelis, 2011). Cell invasion requires the integration of multiple cellular processes, including attachment to BM, remodeling of the actin cytoskeleton, and physical breaching of BM barriers (Rowe and Weiss, 2008; Yilmaz and Christofori, 2009). Microarray studies comparing noninvasive and invasive tumor cells have revealed extensive gene expression changes associated with acquisition of an invasive phenotype (Ramaswamy et al., 2003; van 't Veer et al., 2002; Wang et al., 2002). The transcription factors that regulate these gene expression changes are poorly understood, however, owing to the experimental inaccessibility of the tissues in which invasion occurs and the difficulty of recapitulating this complex cellular behavior *in vitro* (Wang et al., 2005).

An *in vivo* model of invasion across BM that allows for genetic and cell biological analysis at single-cell resolution is anchor cell (AC) invasion into the vulval epithelium in *C. elegans* (Sherwood and Sternberg, 2003). The AC is a specialized uterine cell that invades across BM during larval development to connect the uterine and vulval tissues and generate an opening for mating and embryo passage. AC invasion recapitulates key events in vertebrate cell invasion, including integrin receptor activity, chemotactic signaling, and cytoskeletal polarization (Hagedorn et al., 2009; Ziel et al., 2009). AC invasion is regulated by the bZIP transcription factor FOS-1A (Sherwood et al., 2005), the *C. elegans* ortholog of the Fos family of transcription factors. Fos proteins regulate invasion in *Drosophila* imaginal disc tumors (Uhlirova and Bohmann, 2006) and in vertebrate *in vitro* models of breast (Luo et al., 2010), lung (Adiseshaiah et al., 2008), and adenocarcinoma metastasis (Kustikova et al., 1998), suggesting that Fos proteins are conserved components of an invasive-cell transcriptional network. Other transcription factors appear to function in parallel to FOS-1A during AC invasion, as a small percentage of animals harboring a putative null mutation of *fos-1a* are still able to invade in a delayed manner (Sherwood et al., 2005).

* Corresponding author at: Dept. of Biology, Duke University, Box 90338, Science Drive, Durham, NC 27708.
E-mail address: david.sherwood@duke.edu (D.R. Sherwood).

0012-1606/$ – see front matter © 2011 Elsevier Inc. All rights reserved.
doi:10.1016/j.ydbio.2011.07.012

To identify additional transcriptional regulators of AC invasion, we examined transcription factors with known expression or function in the AC. The basic helix-loop-helix (bHLH) transcription factor HLH-2 is expressed in the AC, where it is required for AC specification prior to the time of invasion (Hwang and Sternberg, 2004; Karp and Greenwald, 2003, 2004). HLH-2 is orthologous to *Drosophila* Daughterless and vertebrate E proteins, class I bHLH transcription factors that bind to E box consensus sites (CANNTG) on target gene promoters (Kee, 2009). A potential role for HLH-2 in AC invasion is suggested by *in vitro* studies showing that E proteins regulate epithelial-mesenchymal transition (EMT), a process in which individual epithelial cells downregulate cell-cell adhesions and acquire invasive capabilities to breach BM (Thiery et al., 2009). The E protein–encoding genes *E2A* and *E2-2* are upregulated *in vitro* in highly invasive carcinoma cells that undergo EMT, and overexpression of *E2A* or *E2-2* in cultured kidney epithelial cells is sufficient to induce EMT (Perez-Moreno et al., 2001; Slattery et al., 2006; Sobrado et al., 2009). Whether E proteins regulate EMT and cell invasion *in vivo* is unknown.

Using RNAi feeding and an *hlh-2* hypomorphic allele to deplete HLH-2 function in the AC during the time of invasion, we show here that HLH-2 regulates AC invasion through a transcriptional pathway that has both independent and overlapping functions with FOS-1A. We identify three genes that are transcriptionally regulated by HLH-2 during invasion: the protocadherin *cdh-3*, and the genes encoding the secreted extracellular matrix proteins *mig-6/papilin* and *him-4/hemicentin*. Reduction of HLH-2 function also decreases the concentration of F-actin at the invasive membrane, indicating a role in regulating cytoskeletal polarity. These results identify HLH-2 as a regulator of cell invasion and expand our understanding of transcriptional pathways acting in invasive cells.

Methods

Worm handling and strains

Animals were reared under standard conditions at 15 °C, 20 °C, or 25 °C (Brenner, 1974). Wild-type nematodes were strain N2. In the text and figures, we designate linkage to a promoter by using the (>) symbol and linkages that fuse open reading frames by using the (::) annotation. The following transgenes and alleles were used in these studies: *qyIs72 [cdc-37::GFP], qyIs92 [hda-1::YFP], qyIs96 [cacn-1>GFP], qyIs91 [egl-43>GFP], qyIs103 [fos-1a>rde-1], qyIs176 [zmp-1>mCherry::moeABD], qyIs142 [GFP::hlh-2], sIs14164 [mig-6>GFP], qyEx112 [unc-62>rde-1::GFP];* **LGI**: *hlh-2(tm1768), unc-40(e271), dpy-5(e907), muIs27 [GFP::mig-2];* **LGII**: *qyIs17* [*zmp-1>mCherry*], *rrf-3(pk1426);* **LGIII:** *unc-119(ed4), syIs129 [him-4-ΔSP::GFP];* **LGIV:** *unc-24(e138), lin-3(n1059), dpy-20(e1282), lin-3(n378), let-59(s49), unc-22(s7), qyIs10 [lam-1::GFP], qyIs15 [zmp-1>HA-βtail],, syIs107 [lin-3>GFP];* **LGV:** *rde-1(ne219), fos-1(ar105); qIs56 (lag-2>GFP);* **LGX:** *syIs50* [*cdh-3>GFP]; syIs123 [fos-1a::YFP], unc-6(ev400).*

The putative hypomorphic allele *hlh-2(tm1768)* has a deletion of 93 amino acids at residues 36–128 and an insertion of six amino acids at the deleted region. The allele is fully sterile at 25 °C and partially sterile at 20 °C (Chesney et al., 2009). Invasion defects in the strain were not temperature sensitive. In genetic crosses, *hlh-2(tm1768)* was followed by sterility at 20 °C and 25 °C and by PCR primers that flanked the deleted region: 5′: gcggatccaaatagccaac; 3′: gagtggaccatttcatttcaag.

RNA interference

Double-stranded RNA (dsRNA)-mediated gene interference (RNAi) was performed by feeding larvae with bacteria expressing dsRNA using standard procedures. dsRNA targeting *hlh-2* was delivered by feeding to either newly hatched larvae in the early-L1 stage ($L1_E$ plating), to larvae grown for 12 h at 15 °C on OP50 bacteria to the mid-to-late L1 stage ($L1_L$ plating), or to larvae grown for 24 h at 15 °C on OP50 to approximately the time of the L1/L2 molt ($L2_M$ plating). Animals grown on OP50 were moved onto *hlh-2* RNAi feeding plates by washing 3× in ddH_2O and 1× in M9 buffer to remove residual OP50. dsRNA constructs for *hlh-2, mep-1, lin-3, lag-2* and *fos-1* were in vector L4440 and were obtained from Open Biosystems (Huntsville, AL). *hlh-2* dsRNA targeted the full 1200-bp open reading frame. Two non-overlapping dsRNA constructs matching 500 bp at either the 5′ or 3′ ends of the *hlh-2* open reading frame were PCR amplified from cDNA and cloned into L4440. cDNA clones were sequenced to verify correct insert. To examine potential off-target RNAi effects, the three *hlh-2* dsRNA constructs were analyzed using the program dsCheck, which scans known coding regions in the *C. elegans* genome for 19-bp matches to dsRNA targeting constructs (Naito et al., 2005). Only the *hlh-2* coding region matched all three *hlh-2* dsRNA constructs.

Uterine- and vulval-specific RNAi experiments were conducted by expressing *rde-1* under the control of the *fos-1a* or *unc-62* promoters, respectively, in an *rde-1(ne219)* mutant animal, as described elsewhere (Ihara et al., 2011; Matus et al., 2010). *fos-1a* expression initiates in the uterine cells in the mid-to-late L2 stage (Sherwood et al., 2005), and *unc-62* expression initiates in the vulval precursor cells in the mid-L2 stage (Ihara et al., 2011).

Generation of GFP::hlh-2

To generate the translational reporter *GFP::hlh-2* (*qyIs174*), *hlh-2* genomic DNA was PCR amplified from the start ATG through the 3′ UTR. This DNA fragment was fused in-frame to the C-terminus of *GFP* DNA (PCR amplified from the vector pPD95.81) using PCR fusion (Hobert, 2002). An 8-kb fragment of *hlh-2* promoter DNA was PCR amplified from genomic DNA and fused to *GFP::hlh-2* to generate the translational reporter.

Microscopy, image acquisition, processing, and analysis

Images were acquired using either a Zeiss AxioImager A1 microscope with a 100× plan-apochromat objective and a Zeiss AxioCam MR charge-coupled device camera, controlled by Zeiss Axiovision software (Zeiss Microimaging, Inc., Thornwood, NJ), or with a Yokogawa spinning disk confocal mounted on a Zeiss AxioImager A1 microscope using iVision software (Biovision Technologies, Exton, PA). Images were processed in ImageJ (NIH Image) and overlaid using Photoshop CS3 (Adobe Systems Inc., San Jose, CA). Z-stack projections were generated using IMARIS 6.0 (Bitplane, Inc., Saint Paul, MN).

Scoring of AC invasion and number of ACs

AC invasion was scored by examining the integrity of the phase-dense line separating the AC from the underlying P6.p-derived vulval precursor cells as previously described (Sherwood et al., 2005). Partial invasion was scored if the hole in the BM at the P6.p four-cell stage was narrower than the width of the AC nucleus. A one-tailed Fisher's exact test was used in Table 1 to determine if the presence of *hlh-2* RNAi or *hlh-2(tm1768)* increased invasion defects relative to animals with wild-type *hlh-2*. In the Fisher's test, the number of full or partially invaded ACs was compared to the number of blocked ACs. The number of ACs in Supplemental Fig. 1 was scored by counting *zmp-1>mCherry*–expressing cells at the P6.p four-cell stage. *zmp-1* was used as the promoter because HLH-2 transcriptionally regulates *cdh-3*, the other commonly used promoter that drives AC-specific expression.

Scoring of polarity and fluorescence intensity

Cytoskeletal polarity was determined by quantifying the ratio of the average fluorescence intensity from a five-pixel-wide linescan drawn along the invasive and noninvasive membranes of Z-stack

Please cite this article as: Schindler, A.J., Sherwood, D.R., The transcription factor HLH-2/E/Daughterless regulates anchor cell invasion across basement membrane in *C. elegans*, Dev. Biol. (2011), doi:10.1016/j.ydbio.2011.07.012

Table 1
Genetic determination of *hlh-2* function in AC invasion.

		ACs showing full, partial, or no invasion[a]							
		P6.p four-cell stage (mid-to-late L3)				P6.p eight-cell stage (early-L4)			
Genotype	**RNAi**	**% full invasion**	**% partial invasion**	**% no invasion**	**n**	**% full invasion**	**% partial invasion**	**% no invasion**	**n**
Wild-type(N2)	L4440 (vector)	100	0	0	100	100	0	0	112
N2	*hlh-2*	46	7	47	177†	61	1	38	128†
N2	5′*hlh-2*	49	8	43	72†	70	7	23	30†
N2	3′*hlh-2*	51	6	43	86†	76	0	24	29†
N2	*mig-6*	96	2	2	50	100	0	0	20
qyIs103[fos-1a>rde-1]; rrf-3(pk1426); rde-1	L4440	99	0	1	75	100	0	0	33
qyIs103[fos-1a>rde-1]; rrf-3(pk1426); rde-1	*hlh-2* ($L1_E$)	62	0	38	58†	83	0	17	64†
qyIs103[fos-1a>rde-1]; rrf-3(pk1426); rde-1	*hlh-2* ($L2_M$)	57	0	43	35†	92	0	8	26
qyEx112[unc-62>rde-1]; rrf-3(pk1426); rde-1	L4440	100	0	0	19	100	0	0	10
qyEx112[unc-62>rde-1]; rrf-3(pk1426); rde-1	*hlh-2*($L1_E$)	100	0	0	18	100	0	0	10
qyEx112[unc-62>rde-1]; rrf-3(pk1426); rde-1	*hbl-1*	60	10	30	20*	100	0	0	10
N2		100	0	0	200	100	0	0	200
hlh-2(tm1768)		95	3	2	184*	100	0	0	62
mig-6(ev701)		100	0	0	20	100	0	0	20
Integrin pathway									
qyIs15[zmp-1>HA-βtail][b]	L4440	0	0	100	15	13	8	79	104
qyIs15[zmp-1>HA-βtail][b]	*hlh-2*	0	0	100	15	2	2	96	66†
Netrin pathway									
unc-6(ev400)	L4440	0	24	76	39	59	11	30	44
unc-6(ev400)	*hlh-2*	0	6	94	47*	26	1	73	68†
hlh-2(tm1768); unc-6(ev400)		0	0	100	18*	7	7	86	41†
unc-40(e271)	*L4440*	14	10	76	42	83	2	15	52
unc-40(e271)	*hlh-2*	2	6	92	48*	32	2	66	44†
FOS-1A pathway									
fos-1(ar105)	L4440	0	0	100	34	1	37	62	75
fos-1(ar105)	*hlh-2*	0	0	100	45	0	13	87	76†
hlh-2(tm1768); fos-1(ar105)		0	0	100	7	2	2	96	42†
Vulval cue									
Vulvaless[c,d]	L4440	14	15	71	66	26	19	55	42
Vulvaless[c,d]	*hlh-2*	7	10	83	98	17	8	75	36*

[a]Full, partial, and no AC invasion was determined by examination under DIC optics of the phase-dense line separating the uterine and vulval tissues. This phase-dense line is formed by an intact BM, and is broken during AC invasion (see Fig. 1B). All *hlh-2* RNAi treatment was $L2_M$ (see Methods) unless indicated otherwise. [b]*qyIs15* [*zmp-1>HA-βtail*] expresses dominant-negative integrin under the AC-specific *zmp-1* promoter. [c]The genotype of the vulvaless mutant strain is *unc-24(e138) lin-3(n1059) dpy-20(e1282)/lin-3(n378) let-59(s49) unc-22(s7)*. [d]Timing of invasion in vulvaless mutants was scored based on gonad arm elongation and number of VU descendants (Sherwood and Sternberg, 2003). Statistics were performed using one-tailed Fisher's exact test by comparing invasion in control conditions (first line of each differently shaded group) to experimental conditions (each additional line of shaded group). Full or partial invasion totals were compared to no invasion animals. *Significant at $p<.05$; †significant at $p<.01$.

projections from ACs expressing GFP::MIG-2 *or zmp-1*>mCherry::moeABD using ImageJ software, as described previously (Hagedorn et al., 2009; Matus et al., 2010). Fluorescence intensities of AC-expressed transcriptional reporters for *zmp-1 (syIs17)*, *cdh-3* (*syIs50*), *lin-3 (syIs107)*, *him-4 (syIs129)*, *egl-43 (qyIs91)*, *lag-2 (qIs56)*, *mig-6 (sIs14164)* and translational reporters for *fos-1a (syIs123)* and *hlh-2 (qyIs174)* were determined using ImageJ software by calculating integrated density (area of AC × mean pixel intensity in that area). In assays that compared fluorescence intensity in control L4440 RNAi-treated animals to intensity in *hlh-2, fos-1,* or *mep-1* RNAi treatments, only animals with blocked AC invasion (indicating effective RNAi treatment) were scored. Statistical significance of RNAi treatments on reporter gene expression or polarity was determined using a two-tailed, unpaired Student's *t*-test.

Results

Overview of AC specification

During the mid-L2 larval stage, one of two equipotent cells, Z1.ppp or Z4.aaa, is specified as the AC by lateral LIN-12/Notch signaling between these cells, with the other cell assuming a ventral uterine (VU) fate (Wilkinson et al., 1994). Following this AC/VU decision, the AC is positioned ventrally in the somatic gonad, separated from the underlying primary-fated vulval precursor cell (1° VPC), P6.p, by the gonadal and ventral epidermal BMs (Fig. 1A). In response to UNC-6 (netrin) signaling from the ventral nerve cord, the netrin receptor UNC-40 (DCC) is polarized to the invasive cell membrane of the AC in contact with BM, where it recruits F-actin, the Rac GTPase MIG-2, and

Please cite this article as: Schindler, A.J., Sherwood, D.R., The transcription factor HLH-2/E/Daughterless regulates anchor cell invasion across basement membrane in *C. elegans*, Dev. Biol. (2011), doi:10.1016/j.ydbio.2011.07.012

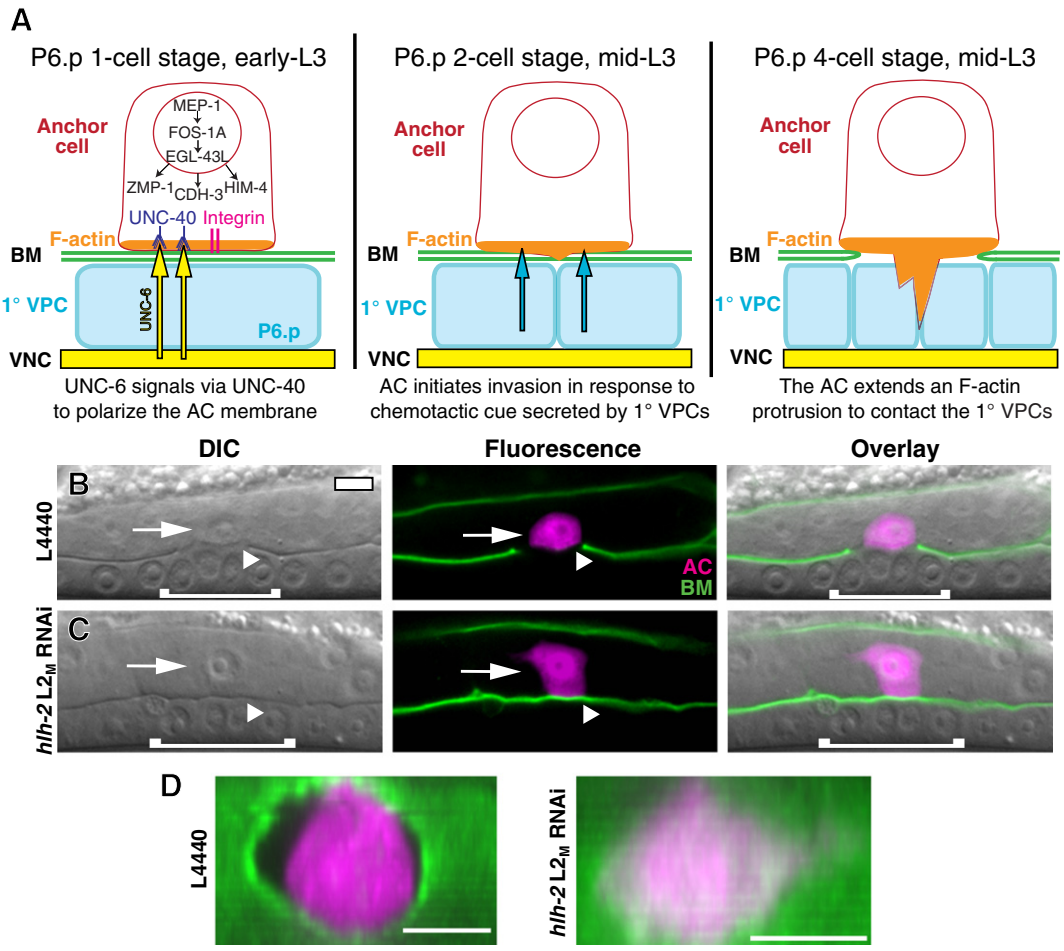

Fig. 1. HLH-2 regulates AC invasion. (A) Schematic diagram depicting AC invasion. After the AC/VU decision, the AC is separated from the underlying P6.p 1°-fated vulval precursor cell (1° VPC) by gonadal and ventral epidermal BMs (green). UNC-6 (netrin) signaling (yellow) from the ventral nerve cord (VNC) polarizes its receptor, UNC-40 (blue), to the ventral surface, where it recruits F-actin and actin regulators (orange). Localization of UNC-40 requires the PAT-3/INA-1 integrin receptor complex (magenta). The transcription factors MEP-1, FOS-1A and EGL-43L regulate transcription of three genes: the zinc metalloprotease *zmp-1*, the protocadherin *cdh-3*, and the extracellular matrix protein *him-4*. At the P6.p two-cell stage (middle panel), in response to a secreted cue from the 1° VPCs (teal), the AC initiates invasion. At the P6.p four-cell stage (right panel), the BMs below the AC are removed and an F-actin-rich protrusion extends between the central 1° VPCs. Details in the left panel are omitted in the center and right panels. (B) Differential interference contrast (DIC) (left), fluorescence (center), and overlaid images (right) of a control L4440 RNAi-treated animal in the mid-L3 larval stage. The AC (arrow, expressing *zmp-1*>*mCherry* in magenta) has invaded through the BM (arrowhead, expressing a translational reporter for the laminin β subunit, LAM-1::GFP, in green). In DIC images, the BM appears as a phase-dense line separating the AC and P6.p-derived VPCs. (C) The BM remains intact following *hlh-2* $L2_M$ RNAi treatment at the L1/L2 molt. Arrowhead points to the unbroken BM, which indicates a failure to invade. (D) Ventral view of ACs in control and *hlh-2* $L2_M$ RNAi-treated animals at the P6.p four-cell stage. Fluorescence images from (B) and (C) (center panels) were rotated clockwise (toward the page) to expose the BMs. In all images, anterior is left and ventral down. White brackets correspond to 1° VPCs. The scale bar represents 5 μm in this and all other figures.

other actin regulators (Ziel et al., 2009). UNC-40 localization is dependent on the INA-1/PAT-3 integrin receptor complex, which also polarizes to the invasive cell membrane (Fig. 1A) (Hagedorn et al., 2009). Following the first cell division of P6.p in the mid-L3 stage (P6.p two-cell stage), the AC initiates invasion in response to an unknown chemotactic cue secreted by the 1°-fated VPCs (Sherwood and Sternberg, 2003). The ability of the AC to breach the BM in response to the vulval cue is dependent on the C2H2 zinc-finger transcription factor MEP-1, the bZIP transcription factor FOS-1A, and the zinc-finger transcription factor EGL-43L, which function in a hierarchical pathway to promote the expression of *zmp-1*, *cdh-3*, and *him-4*, genes encoding a zinc matrix metalloproteinase, a protocadherin and an extracellular matrix protein, respectively, which are thought to act with unknown targets to breach the BM (Hwang et al., 2007; Matus et al., 2010; Rimann and Hajnal, 2007; Sherwood et al., 2005). AC invasion is synchronized tightly with the underlying 1° VPCs, and invariantly completes invasion at the P6.p four-cell stage in the mid-to-late L3 larval stage (Fig. 1A) (Sherwood and Sternberg, 2003).

The transcription factor HLH-2 is required for AC invasion

HLH-2 has previously been shown to act at two distinct steps in AC specification prior to invasion (Karp and Greenwald, 2003, 2004). First, it endows Z1.ppp and Z4.aaa with the capacity to be specified as an AC. Treatment with *hlh-2* RNAi in the early-L1 stage ($L1_E$ RNAi, see Methods for RNAi treatment terminology) causes both Z1.ppp and Z4.aaa to assume the VU identity, as determined by lineage analysis and by the absence of an AC-expressed reporter, *zmp-1*>*mCherry* (Fig. S1; Karp and Greenwald, 2004). After pro-AC specification, HLH-2 later regulates the AC/VU decision through direct transcriptional activation of *lag-2* (*Delta*), the LIN-12/Notch ligand, which is expressed by the presumptive AC and signals laterally via LIN-12 localized on the presumptive VU to suppress AC fate (Karp and Greenwald, 2003). *hlh-2* RNAi treatment in the late-L1 stage ($L1_L$ RNAi) causes both Z1.ppp and Z4.aaa to assume the AC identity (Fig. S1; Karp and Greenwald, 2003, 2004). HLH-2 also has a later role in formation of the uterine seam cell (UTSE), a multinucleate syncytium whose formation requires an inductive signal from the AC (Karp and Greenwald, 2004).

Please cite this article as: Schindler, A.J., Sherwood, D.R., The transcription factor HLH-2/E/Daughterless regulates anchor cell invasion across basement membrane in *C. elegans*, Dev. Biol. (2011), doi:10.1016/j.ydbio.2011.07.012

To test for a possible role for *hlh-2* in AC invasion after the AC/VU decision, we grew animals to approximately the time of the L1/L2 molt before moving them on to *hlh-2* RNAi feeding plates ($L2_M$ RNAi). In this treatment, 72% of animals had a single AC expressing *zmp-1>mCherry*, 9% displayed the $L1_E$ no AC phenotype and 19% displayed the $L1_L$ two AC phenotype (Fig. S1). Given the lag between dsRNA feeding and mRNA depletion, it appears that sufficient amounts of *hlh-2* mRNA remain during the mid-L2 stage for the AC/VU decision to be properly executed in the majority of animals treated with *hlh-2* $L2_M$ RNAi. To examine possible defects in AC invasion caused by depletion of *hlh-2* after the AC/VU decision, we performed *hlh-2* $L2_M$ RNAi on animals expressing a full-length translational reporter for the β subunit of the BM protein laminin (LAM-1::GFP) (Kao et al., 2006). In control animals treated with L4440 empty-vector RNAi, the BM under the AC was removed by the P6.p four-cell stage (Fig. 1B; Table 1). In contrast, animals treated with *hlh-2* $L2_M$ RNAi often had intact LAM-1::GFP (Fig. 1C–D). Scoring these animals for invasion revealed that *hlh-2* $L2_M$ RNAi-treated animals had a 54% defect in invasion at the P6.p four-cell stage, and a 39% defect one cell division later at the P6.p eight-cell stage in the early-L4 larval stage (Table 1). To avoid complications with defects possibly caused by an inability to execute the AC/VU decision, only animals with a single, *zmp-1*–expressing AC were scored for invasion. In *hlh-2* RNAi experiments, the dsRNA was targeted against the full 1200-bp *hlh-2* coding region. As controls, two dsRNA constructs targeting non-overlapping 500-bp segments at either the 5′ or 3′ ends of the *hlh-2* open reading frame were generated, and produced similar invasion blocks, ruling out possible off-target effects (Table 1). We also examined AC invasion in animals homozygous for *hlh-2(tm1768)*, a likely hypomorphic allele, which contains a deletion of 93 amino acids near the N-terminus and an insertion of six amino acids in the deleted region (Chesney et al., 2009). We found a significant 5% defect in AC invasion at the P6.p four-cell stage in *hlh-2(tm1768)* (Table 1; Fig. S2). *hlh-2(tm1768)* animals with zero or two ACs were not observed (>200 animals), suggesting that the lesion in *hlh-2(tm1768)* specifically affects a process related to AC invasion.

We next wanted to assess the degree to which the AC was properly differentiated after reduction of *hlh-2* function after the AC/VU decision. A differentiated AC can be distinguished by its morphology under DIC optics and by a suite of genes that are expressed in an AC-specific manner. Animals treated with *hlh-2* $L2_M$ RNAi had a characteristic AC morphology (granular vesicles in the cytoplasm and smaller nucleolus than other uterine cells), and were similar in size to ACs in control RNAi-treated animals (Fig. 1B–C; Fig. S3). Two observable differences in AC morphology in *hlh-2* $L2_M$ RNAi-treated animals were that AC nuclei were often positioned more dorsally in the somatic gonad, and ACs were more rectangular than the rounded shape seen in control animals (Fig. 1B–C; Fig. S3). We next examined the expression of several AC-specific reporter genes. Expression of *zmp-1>mCherry*, which is turned on in the AC after the AC/VU decision, was equivalent in control and *hlh-2* $L2_M$ RNAi-treated animals with blocked invasion (Fig. 1B–C; Fig. 5A). Four other genes upregulated in the AC—the HSP90 co-chaperone *cdc-37*, the Rac GTPase *mig-2*, the histone deacetylase *hda-1*, and *cacn-1*, an ortholog of *Drosophila cactin* (Matus et al., 2010)—were also expressed normally following *hlh-2* $L2_M$ RNAi treatment, and were not expressed at elevated levels in the VU cells (Fig. S3). Although other aspects of AC differentiation are possibly perturbed by *hlh-2* $L2_M$ RNAi treatment, these results demonstrate that several hallmarks of AC differentiation are normal following depletion of *hlh-2* at a time after the AC/VU decision.

HLH-2 is expressed in the AC during specification and invasion

To determine the HLH-2 expression pattern prior to and during the time of AC invasion, we generated a translational reporter containing 8 kb of *hlh-2* promoter DNA fused to the full-length *hlh-2* coding region and 3′ UTR, tagged at the N-terminus with GFP. In the somatic gonad, GFP::HLH-2 was expressed at low levels in the Z1/Z4 somatic gonadal precursor cells at the L1 stage. This is consistent with HLH-2 being required for specification and function of the AC and DTCs, the descendants of Z1/Z4 (Chesney et al., 2009; Karp and Greenwald, 2004) (Fig. 2A; Fig. S1). During the time of the AC/VU decision, GFP::HLH-2 was expressed in both pre-AC and pre-VU cells (Fig. 2B), and after the AC/VU decision, GFP::HLH-2 was reduced in the VU and its descendants (Fig. 2C), as shown previously by HLH-2 immunolocalization (Karp and Greenwald, 2003). GFP::HLH-2 persisted in the AC through the time of invasion (Fig. 2D), suggesting a cell-autonomous function for HLH-2 in regulating AC invasion. Although GFP::HLH-2 was present in the VU cells at reduced levels during the time of invasion, the AC is the likely site of HLH-2 function, since laser ablation of the uterine cells surrounding the AC does not inhibit invasion (Ihara et al., 2011; Sherwood and Sternberg, 2003). To determine the specificity of the *hlh-2* RNAi treatment, we treated animals expressing integrated *GFP::hlh-2* with *hlh-2* $L2_M$ RNAi. The reporter was downregulated in animals in which invasion was blocked, demonstrating the correlation between RNAi depletion of *hlh-2* and invasion defects (Fig. 2E). Notably, GFP::HLH-2 was not expressed in the 1° VPCs, supporting the AC as the site of action for *hlh-2* in AC invasion.

AC invasion requires the coordinated action of the AC and the underlying 1° VPCs, which secrete a chemotactic cue that stimulates invasion. We further examined *hlh-2* site-of-action using uterine (*fos-1a>rde-1*) and vulval-specific (*unc-62>rde-1*) RNAi strains (Hagedorn et al., 2009; Ihara et al., 2011; Matus et al., 2010). In these experiments, animals possess a null mutation of *rde-1*, a gene required for RNAi sensitivity (Tabara et al., 1999). A functional copy of *rde-1* is expressed specifically in a tissue of interest, thus restoring RNAi in those cells and allowing for a determination of site-of-action. The uterine-specific strain (*fos-1a>rde-1*) is sensitive to RNAi after *fos-1a* initiates expression in the mid-to-late L2 stage, after the AC/VU decision but prior to invasion (Sherwood et al., 2005). Consistent with this timing, *hlh-2* $L1_E$ RNAi feeding, which in wild-type animals causes both Z1.ppp and Z4.aaa to assume the VU fate (Fig. S1), did not display defects in AC/VU specification, but caused a 38% defect in invasion at the P6.p four-cell stage. *hlh-2* $L2_M$ RNAi treatment caused a similar invasion defect (Table 1). In contrast, *hlh-2* $L1_E$ RNAi did not cause invasion defects in a strain (*unc-62>rde-1)* in which RNAi sensitivity is restored in the vulval precursor cells during the mid-L2 larval stage (Ihara et al., 2011) (Table 1). A control RNAi targeting *hbl-1* (*hunchback*), which controls the timing of vulval cell divisions and thus the vulval cue (Matus et al., 2010), caused invasion defects at the P6.p four-cell stage in *unc-62>rde-1* animals (Table 1). Taken together, these results provide evidence that HLH-2 acts in the AC to promote invasion.

HLH-2 represents a novel transcriptional pathway in AC invasion

We next examined if HLH-2 functions in any of the major pathways that regulate AC invasion (Fig. 1A). To test this, we performed genetic analysis experiments using both *hlh-2* $L2_M$ RNAi and *hlh-2(tm1768)* mutant animals. We first examined interactions with the integrin pathway. We could not test interactions with a null mutant in either gene in the integrin receptor complex, as loss-of-function of the α subunit (*ina-1*) or the β subunit (*pat-3*) are embryonic or early larval lethal. Instead, we used animals stably expressing dominant-negative *pat-3* in the AC under control of the *zmp-1* promoter, which appears to strongly inhibit integrin function in the AC (Hagedorn et al., 2009). Although definitive conclusions of genetic interactions cannot be drawn without a null allele of *ina-1* or *pat-3*, treatment with *hlh-2* $L2_M$ RNAi significantly increased the invasion defect in animals expressing dominant-negative *pat-3*, consistent with the possibility that HLH-2 has functions outside of integrin signaling during invasion (Table 1). To examine interactions with the UNC-6/UNC-40 netrin pathway, we fed *hlh-2* $L2_M$ dsRNA to the null mutants *unc-6(ev400)* (netrin ligand) and *unc-40(e271)* (netrin receptor), and found that it significantly increased

Please cite this article as: Schindler, A.J., Sherwood, D.R., The transcription factor HLH-2/E/Daughterless regulates anchor cell invasion across basement membrane in *C. elegans*, Dev. Biol. (2011), doi:10.1016/j.ydbio.2011.07.012

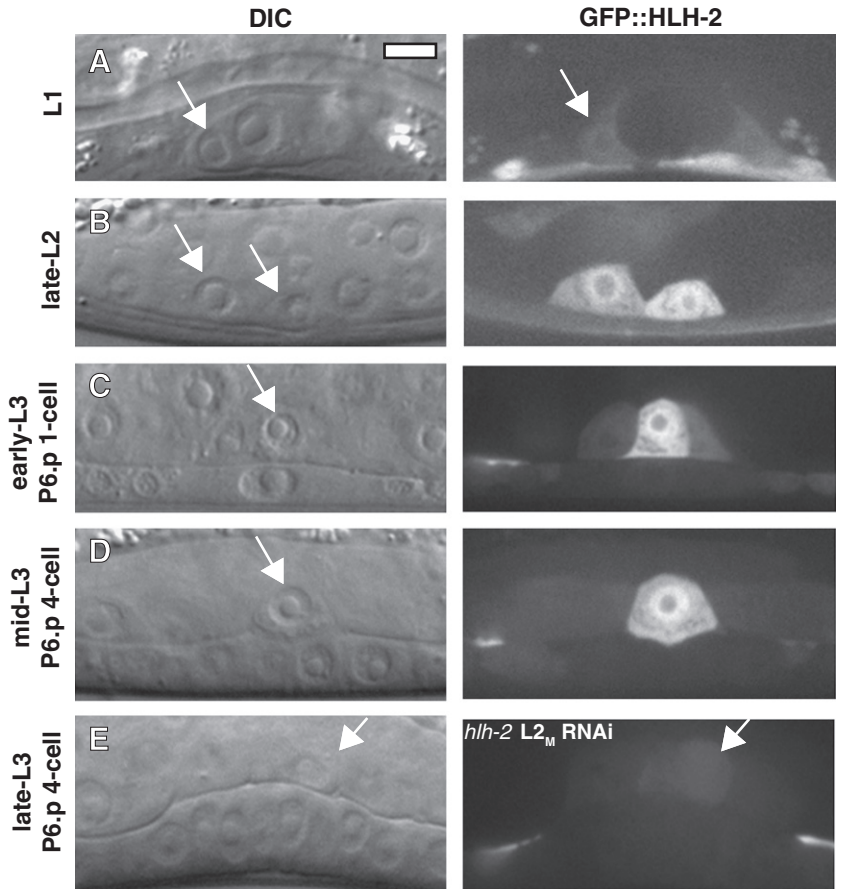

Fig. 2. HLH-2 is expressed in the AC during specification and invasion. DIC images (left in each lettered pair) and corresponding fluorescent images (right in each lettered pair) of animals expressing a translational GFP::HLH-2 reporter. (A) GFP::HLH-2 is expressed at low levels in the Z1/Z4 somatic gonadal precursor cells (SGPs) in the L1 stage. Arrow points to one of two SGPs. (B) GFP::HLH-2 is expressed in the AC and VU cells (arrows) in the late-L2 stage, but the AC (right cell) has higher fluorescence. (C) In the early-L3 stage, following the AC/VU decision, GFP::HLH-2 is reduced in the VU cell, whereas fluorescence remains elevated in the AC. Arrow points to the AC, positioned above the P6.p 1° VPC. The expression pattern in (B–C) is similar to that shown previously by anti-HLH-2 immunolocalization (Karp and Greenwald, 2003). (D) In the mid-L3 stage, GFP::HLH-2 is expressed in the AC during the time of invasion. (E) GFP::HLH-2 is strongly reduced at the late-L3 stage in an animal treated with *hlh-2* $L2_M$ RNAi that caused a block in invasion.

the invasion defect in both mutants at the four- and eight-cell P6.p stages. Animals doubly mutant for *unc-6(ev400)* and *hlh-2(tm1768)* also had a significantly greater invasion defect than *unc-6(ev400)* animals alone (Table 1). These results indicate that HLH-2 has functions outside the UNC-6/UNC-40 netrin pathway. We next examined the genetic interaction between *hlh-2* and *fos-1a*. *hlh-2* $L2_M$ RNAi treatment of *fos-1 (ar105)* null mutants and animals doubly mutant for *hlh-2(tm1768)* and *fos-1(ar105)* had defects significantly greater than in *fos-1(ar105)* alone (Table 1). Finally, we tested interactions with the vulval cue using a vulvaless mutant strain. Treatment with *hlh-2* $L2_M$ RNAi increased the invasion defect in vulvaless animals significantly at the P6.p eight-cell stage (Table 1), indicating that HLH-2 has functions outside of the vulval cue pathway. Taken together, these results indicate that HLH-2 does not function exclusively in any of the major identified AC invasion pathways.

LIN-3 and LAG-2 do not mediate HLH-2 function during AC invasion

We next sought to identify downstream effectors of HLH-2 during AC invasion. Two genes whose expression is known to be regulated by HLH-2 in the AC are *lin-3* (EGF) and *lag-2* (Delta) (Hwang and Sternberg, 2004; Karp and Greenwald, 2003). LIN-3 is secreted from the AC and induces P6.p to adopt the 1° VPC fate. In the absence of *lin-3*, P6.p adopts the 3° VPC fate and divides only once. Tertiary-fated VPCs do not generate the vulval cue, causing defects in AC invasion (Sherwood and Sternberg, 2003). We first examined *lin-3>GFP* expression and found a 78% reduction in fluorescence intensity following *hlh-2* $L2_M$ RNAi treatment (Fig. 3A–B), consistent with previous results (Hwang and Sternberg, 2004). Despite this reduction in expression, the 1° VPC fate was specified in P6.p and its descendants following *hlh-2* $L2_M$ RNAi treatment that blocked invasion, as determined by expression of the 1° fate marker *egl-17>GFP* and by normal morphological development of the VPCs (Fig. 3C–D). These results suggest that HLH-2 does not regulate invasion through specification of the 1° VPC fate. We next asked if depletion of *lin-3* during the time of AC invasion phenocopied depletion of *hlh-2*. The majority of animals (40/54) treated with *lin-3* $L2_M$ RNAi had defects in 1° VPC fate specification: *egl-17>GFP* was not expressed and VPC cell division was aberrant (Fig. 3E). In animals that failed to specify the 1° VPC fate, invasion was defective (18/40 failed to invade), consistent with loss of the vulval cue. In *lin-3* $L2_M$ RNAi-fed animals in which the 1° VPC fate was specified, invasion was normal (14/14 invaded, P6.p four-cell stage). These results suggest that *lin-3* does not have a separate role in AC invasion beyond its role in specifying VPC fates. Thus, HLH-2 does not appear to regulate invasion through *lin-3* expression.

We next asked if *lag-2*, which acts downstream of HLH-2 during the AC/VU decision (Karp and Greenwald, 2003), also mediated HLH-2 effects on AC invasion. Expression of a *lag-2>GFP* reporter was comparable in control RNAi-treated animals and *hlh-2* $L2_M$ RNAi-treated animals with defects in invasion (Fig. 3F–G), suggesting that *lag-2* is not regulated by HLH-2 during invasion. We further tested *lag-2* for a role in invasion using *lag-2* RNAi feeding. No invasion block was observed (20/20 invaded, P6.p four-cell stage), despite the presence of

Please cite this article as: Schindler, A.J., Sherwood, D.R., The transcription factor HLH-2/E/Daughterless regulates anchor cell invasion across basement membrane in *C. elegans*, Dev. Biol. (2011), doi:10.1016/j.ydbio.2011.07.012

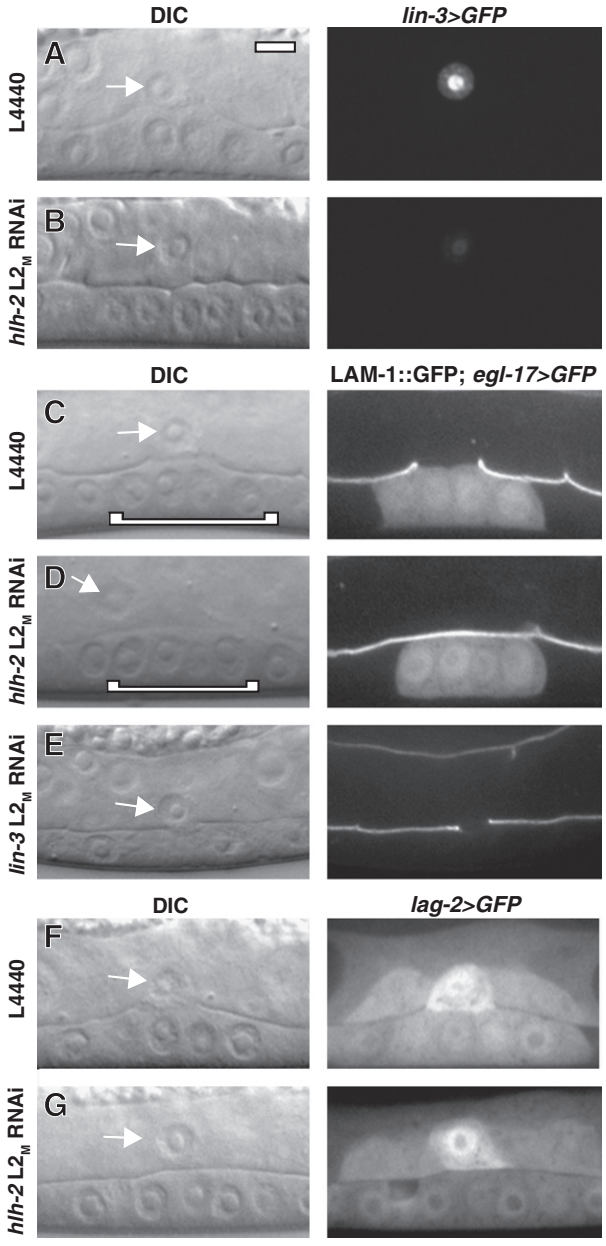

Fig. 3. LIN-3 and LAG-2 do not regulate invasion downstream of HLH-2. DIC images (left in each lettered pair) and corresponding fluorescence images (right in each lettered pair). Control L4440 (A) and *hlh-2* $L2_M$ RNAi treatment (B) in animals expressing *lin-3>GFP* transcriptional reporter. Expression is reduced 78% by *hlh-2* $L2_M$ RNAi treatment compared to control RNAi ($n = 12$, $p < .01$). Control L4440 (C) and *hlh-2* $L2_M$ RNAi treatment (D) in animals expressing LAM-1::GFP and *egl-17>GFP*, a marker for the 1° VPC fate. In the DIC images, 1° VPCs are indicated with a white bracket. 1° VPC fate is specified in animals with blocked invasion following *hlh-2* $L2_M$ RNAi treatment. (E) *lin-3* $L2_M$ RNAi treatment causes loss of 1° VPC fate specification, as indicated by absence of *egl-17>GFP* and by vulval morphology defects. Despite loss of 1° VPC fate, the AC still partially invades at the late-L3 stage. (F) Control L4440 and (G) *hlh-2* $L2_M$ RNAi treatment in animals expressing *lag-2>GFP* transcriptional reporter. Expression is comparable in the two conditions ($n = 11$, $p = .84$).

two ACs in 65% (13/20) of animals (evidence that the RNAi treatment reduced *lag-2* function). This contrasts with *hlh-2* RNAi treatment, where invasion was never observed in animals with two ACs (0/50 invaded, P6.p four-cell stage; Fig. S1). We conclude that *lag-2* does not function downstream of HLH-2 to regulate AC invasion.

HLH-2 is partially regulated by FOS-1A and MEP-1

The genetic results suggest that HLH-2 has functions outside of the FOS-1A transcriptional pathway during invasion (Table 1), but do not exclude a role in regulating this pathway. To determine if HLH-2 regulates the FOS-1A pathway, we fed *hlh-2* $L2_M$ RNAi to animals expressing reporters for *fos-1a* and its downstream target gene, *egl-43L* (Hwang et al., 2007; Rimann and Hajnal, 2007). We found no significant difference in the expression of FOS-1A::YFP or *egl-43L>GFP* in animals with blocked invasion (Fig. S4). We next examined regulation of HLH-2 by FOS-1A. AC expression of GFP::HLH-2 was reduced 28% by *fos-1* RNAi treatment (Fig. 4A–B). RNAi targeting the transcription factor *mep-1*, which strongly regulates *fos-1a* expression (Matus et al., 2010), reduced GFP::HLH-2 fluorescence to a similar degree as *fos-1* RNAi (Fig. 4C–D), suggesting that MEP-1 regulates GFP::HLH-2 indirectly through *fos-1a*. This modest regulation by the FOS-1A transcriptional pathway of HLH-2, and the absence of HLH-2 regulation of the FOS-1A pathway, support the genetic evidence that these transcriptional pathways have separate functions in regulating AC invasion.

HLH-2 converges with FOS-1A to regulate cdh-3, him-4, and mig-6

Transcription factors in gene regulatory networks often function cooperatively in regulation of downstream target genes (Arnone and Davidson, 1997). We asked if FOS-1A and HLH-2 might converge to regulate AC-expressed genes by examining the expression of the three known transcriptional targets of the FOS-1A pathway in the AC: the matrix metalloproteinase *zmp-1*, the protocadherin *cdh-3*, and the secreted extracellular matrix protein *him-4*. Treatment with *hlh-2* $L2_M$ RNAi did not significantly reduce expression of a *zmp-1* reporter, which is strongly regulated by FOS-1A (Sherwood et al., 2005) (Fig. 1; Fig. 5A); however, *cdh-3* reporter expression was reduced in animals with blocked invasion by 32% (Fig. 5A–C), and *him-4* reporter expression was reduced by 90% (Fig. 5A,D–E). These results demonstrate that HLH-2 converges with FOS-1A on some, but not all, transcriptionally regulated genes.

A previous report (Cram et al., 2006) identified *mig-6*, the *C. elegans* ortholog of the extracellular matrix protein Papilin, as a downstream target of HLH-2 in the distal tip cells (DTCs), where it is required for gonad arm elongation (Kawano et al., 2009). We examined a *mig-6>GFP* transcriptional reporter and found that it is expressed in the AC during the time of invasion (Fig. 6A). *hlh-2* $L2_M$ RNAi treatment reduced detectable expression of *mig-6* almost completely (94%; Fig. 6B). *fos-1* RNAi also reduced *mig-6>GFP* expression, but to a lower level of 57% (Fig. 6C), suggesting an apparent divergence between the two transcriptional pathways. We previously reported an 8% AC invasion defect in animals expressing a *mig-6* hypomorphic allele, *mig-6(ev700)* (Ihara et al., 2011). We further tested a second hypomorphic allele, *mig-6(ev701)*, and found no invasion defect (Table 1). We also depleted *mig-6* by RNAi and found only a single invasion block in 50 animals examined (Table 1). Therefore, despite its presence in the AC and its regulation by HLH-2, reduction of *mig-6* function does not dramatically perturb AC invasion. Taken together, these results identify HLH-2 as a regulator of *mig-6* expression in the AC and indicate that, similar to FOS-1A, HLH-2 regulates multiple genes that may contribute to AC invasion.

HLH-2 regulates polarization of F-actin and Rac GTPase to the AC invasive cell membrane

Following the AC/VU decision, an F-actin–rich domain becomes polarized to the invasive cell membrane of the AC, which is in direct contact with the BM (Fig. 1A). This polarized F-actin is maintained throughout invasion and is thought to be necessary for the AC to generate invasive protrusions in response to the vulval cue (Hagedorn et al., 2009; Ziel et al., 2009). AC polarity has previously been shown to be independent of *fos-1a* expression (Matus et al., 2010; Ziel et al., 2009). To determine if polarity is affected by reduction of HLH-2 function, we examined the cellular localization of an AC-specific F-actin reporter, *zmp-1*>mCherry::moeABD, in which the actin-binding domain of moesin (moeABD) is fused to mCherry and expressed under the

Please cite this article as: Schindler, A.J., Sherwood, D.R., The transcription factor HLH-2/E/Daughterless regulates anchor cell invasion across basement membrane in *C. elegans*, Dev. Biol. (2011), doi:10.1016/j.ydbio.2011.07.012

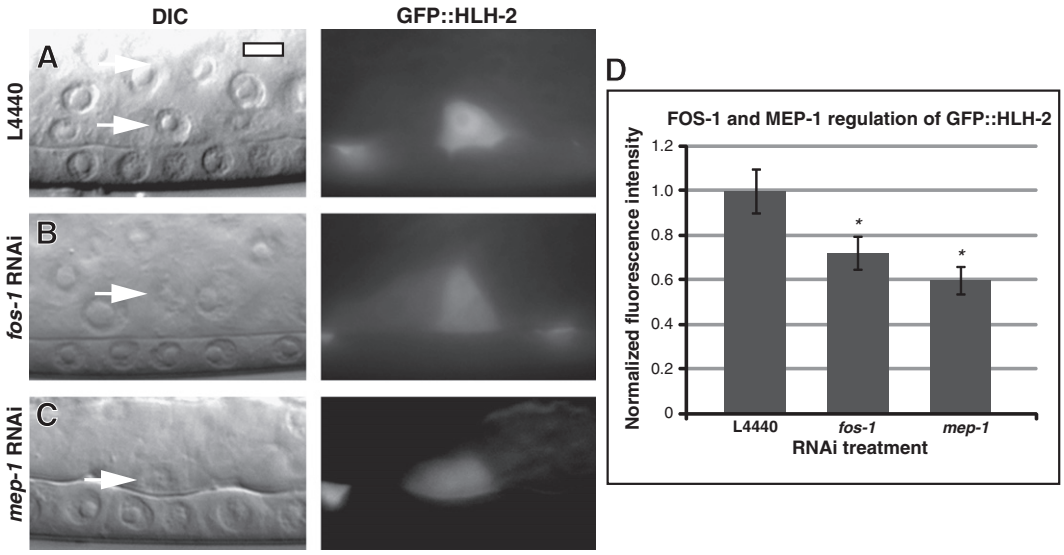

Fig. 4. HLH-2 is partially regulated by FOS-1A and MEP-1. DIC images (left in each lettered pair) and corresponding fluorescent images (right in each lettered pair) of mid-L3 animals expressing a translational GFP::HLH-2 reporter. (A) Control L4440 RNAi, (B) *fos-1* RNAi, and (C) *mep-1* RNAi-treated animals. GFP::HLH-2 fluorescence in the AC is reduced by *fos-1* and *mep-1* RNAi treatment. (D) Quantification of fluorescence intensity from RNAi experiments. $n \geq 15$; *: $p < .05$; error ± S.E.M.

zmp-1 promoter. After treatment with control RNAi, localization of *zmp-1*>mCherry::moeABD was enriched 2.5-fold at the invasive membrane relative to the apico-lateral membrane at the P6.p four-cell stage (Fig. 7A and F). After *hlh-2* $L2_M$ RNAi treatment, *zmp-1*>mCherry::moeABD polarity was reduced by 34%, with ectopic patches of F-actin visible on the apical and lateral sides of the AC (Fig. 7B and F). To complement these experiments, we crossed *zmp-1*>mCherry::moeABD into *hlh-2 (tm1768)* and found a 23% reduction in the polarity ratio compared to that seen in wild-type animals (Fig. 7C and F).

We also examined polarity of a second reporter for the invasive cell membrane, GFP::MIG-2, in which a functional full-length copy of the Rac GTPase MIG-2 fused to GFP is expressed under its own promoter. Treatment with *hlh-2* $L2_M$ RNAi reduced polarity by 40% compared to control RNAi (Fig. 7D–F). This loss of polarity was not a byproduct of a failure to invade, as *hlh-2* $L2_M$ RNAi treatment reduced GFP::MIG-2 polarity by 27% at the P6.p two-cell stage, 2 h prior to full invasion. The cellular localization of GFP::MIG-2 in *hlh-2* $L2_M$ RNAi-treated animals was similar to that of F-actin, with ectopic patches on the lateral sides (Fig. 7E, Fig. S3). The results of the polarity measurements demonstrate that HLH-2 function is required for the normal formation of the invasive cell membrane of the AC.

Discussion

Cell invasion across BM is a critical aspect of cell dissemination in many developmental processes, leukocyte trafficking, and cancer metastasis. The genetic programs that control cell invasion are thought to be conserved, but remain poorly understood (Rowe and Weiss, 2008). We show here that the basic helix-loop-helix transcription factor HLH-2, an ortholog of *Drosophila* Daughterless and vertebrate E proteins, is required for AC invasion in *C. elegans*. Our genetic and cell biological data indicate that HLH-2 has distinct functions from other known regulators of AC invasion, but also overlaps with the FOS-1A transcriptional pathway in regulating AC-expressed genes. Through expression analysis, we identify three genes that are transcriptionally regulated by HLH-2, and show that HLH–2 regulates formation of the AC F-actin–rich invasive cell membrane.

HLH-2 has overlapping and distinct roles from FOS-1A

Adoption of an invasive phenotype is associated with changes in gene expression, including genes thought to mediate critical processes in invasion such as migration, cytoskeletal polarization, and breaching of BM barriers (Ramaswamy et al., 2003; van 't Veer et al., 2002; Wang et al., 2002). Fos family transcription factors regulate invasion in *Drosophila, C. elegans,* and vertebrate *in vitro* invasion models (Ozanne et al., 2007; Sherwood et al., 2005; Uhlirova and Bohmann, 2006). This work suggests that, similar to Fos transcription factors, HLH-2/E proteins may also have conserved roles in cell invasion. E proteins are regulators of EMT, which endows epithelial cells with migratory and invasive capabilities (Perez-Moreno et al., 2001; Slattery et al., 2006; Sobrado et al., 2009). The connection between EMT and gene expression changes associated with invasion has not been established *in vivo*. This work reveals that a conserved transcription factor that regulates EMT also regulates gene expression changes during cell invasion.

HLH-2 regulates overlapping and distinct processes from FOS-1A during AC invasion. Both *hlh-2* $L2_M$ RNAi treatment and the hypomorphic allele *hlh-2(tm1768)* enhance the invasion defect in a *fos-1a* null mutant, indicating that HLH-2 has functions separate from FOS-1A. One possible scenario for the independent functions of the transcription factors is that HLH-2, analogous to transcription factors that regulate EMT, mediates cell shape changes and formation of F-actin–rich protrusions, whereas FOS-1A is devoted more to physical breaching of BM barriers. Consistent with this, HLH-2 is required for proper formation of the AC invasive membrane domain, whereas FOS-1A is not required (Matus et al., 2010; Ziel et al., 2009). In contrast, FOS-1A, but not HLH-2, regulates expression of *zmp-1*, a member of the family of matrix metalloproteases thought to participate in breaching BM during invasion (Rowe and Weiss, 2009; Sherwood et al., 2005). The FOS-1A and HLH-2 pathways do overlap, however, as both transcription factors regulate expression of *cdh-3*, *him-4*, and *mig-6*, and FOS-1A appears to be important for full expression of HLH-2 protein in the AC. The overlapping and independent pathways, summarized in Fig. 8, present a current picture of the AC transcriptional network up to the time of invasion. Additional transcriptional targets of FOS-1A and HLH-2 likely exist, since mutants in *zmp-1, cdh-3, him-4,* and *mig-6* have only modest invasion defects individually or in combination (Sherwood et al., 2005).

The interactive gene regulatory network of the AC mirrors other studied regulatory circuits. For example, during vulval development the transcription factors COG-1, LIN-29, LIN-11, and EGL-38 overlap in the regulation of several molecular targets, and also regulate each other (Inoue et al., 2005; Ririe et al., 2008). In the sea urchin skeletogenic

Please cite this article as: Schindler, A.J., Sherwood, D.R., The transcription factor HLH-2/E/Daughterless regulates anchor cell invasion across basement membrane in *C. elegans*, Dev. Biol. (2011), doi:10.1016/j.ydbio.2011.07.012

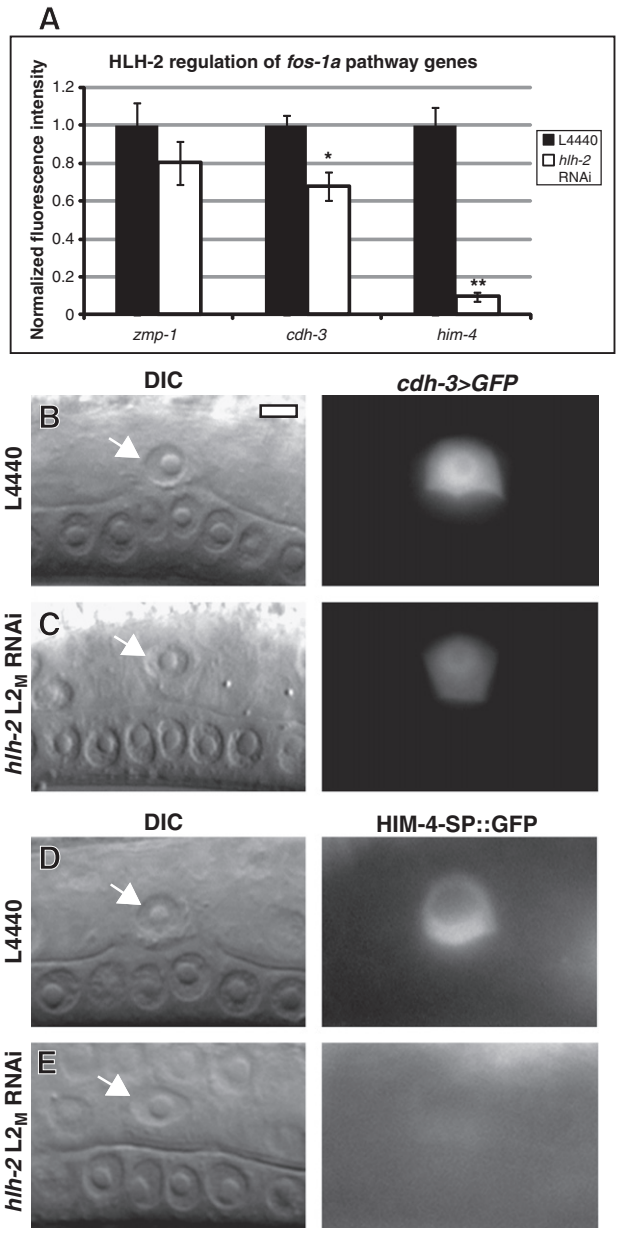

Fig. 5. HLH-2 has parallel functions to FOS-1A in regulating AC-expressed genes. (A) Transgenic animals with fluorescent reporters for *zmp-1*, *cdh-3*, and *him-4* were treated with either control L4440 or *hlh-2* $L2_M$ RNAi. Fluorescence intensity in animals with blocked invasion was quantified and normalized to control values. *cdh-3* expression was reduced by 32%, and *him-4* expression was reduced by 90%. $n \geq 15$; $^{*}p < .05$; $^{**}p < 1 \times 10^{-5}$; error ± S.E.M. (B–E) DIC images (left) and corresponding fluorescence images (right) at the mid-L3 stage of animals expressing either *cdh-3>GFP* (B–C) or HIM-4-ΔSP::GFP (D–E), in which the *him-4* gene lacking the signal sequence is fused to GFP. (B–C) *cdh-3>GFP* expression is moderately reduced by *hlh-2* $L2_M$ RNAi, and (D–E) HIM-4-ΔSP::GFP expression is mostly silenced by *hlh-2* $L2_M$ RNAi.

network, the transcription factors hex, tgif and erg regulate expression of each other and converge in the downstream regulation of the transcription factor FoxO (Oliveri et al., 2008). Other transcription factors will be added to the AC network, as many AC-enriched genes (*e.g., cdc-37*, *mig-2*, and *cactin*) are expressed independently of FOS-1A and HLH-2 (Matus et al., 2010; Sherwood et al., 2005).

HLH-2 regulates expression of extracellular matrix proteins mig-6 and him-4 and the protocadherin cdh-3

We identified three genes regulated by HLH-2 in the AC: *mig-6, him-4,* and *cdh-3*. bHLH transcription factors bind to E-box motifs (CANNTG) in target gene promoters. Although an examination of direct binding by HLH-2 to the gene promoters was not conducted in this study, analysis of the 5′ *cis*-regulatory regions of the three genes shows clusters of three or more E-box motifs in a 100-bp region in the *mig-6* promoter at −700 bp and −2.6 kb from the transcription start site, and in the *him-4* promoter at −1 kb, −2.3 kb, and −3.7 kb. The *cdh-3* promoter contains four E-box sites within a 66-bp span that is located in the AC promoter element, a 1500-bp region required for AC expression (Kirouac and Sternberg, 2003). Homotypic clustering of binding sites specific for a transcription factor increases the probability of binding in that region (Lifanov et al., 2003), raising the possibility that HLH-2 directly binds to the promoters of *mig-6*, *him-4*, and *cdh-3*.

The two genes most strongly regulated by HLH-2 in the AC are *mig-6* and *him-4*, which are reduced in expression ≥90% following *hlh-2* $L2_M$ RNAi. *mig-6 and him-4* are secreted extracellular matrix proteins that can localize to BM (Kawano et al., 2009; Vogel and Hedgecock, 2001). HLH-2 also regulates expression of *mig-6* in the DTCs, as well as a secreted metalloprotease, *gon-1* (Kawano et al., 2009; Tamai and Nishiwaki, 2007). The AC and DTCs share a common lineage and have several functional similarities, including response to netrin and a requirement for integrin receptor signaling (Hedgecock et al., 1990; Lee et al., 2001). Both cell types interact with BM: the AC invades across BM, and the DTCs migrate along BM as it is being deposited. The presence of HLH-2 in the AC and DTCs, and its regulation of secreted proteins in those cells, suggests that HLH-2 may have a specialized role in mediating cell-BM interactions.

HLH-2 is the first transcriptional link between AC invasion and DTC migration (Karp and Greenwald, 2004). FOS-1A and EGL-43 are not known to be required in the DTCs, and DTC-expressed transcription factors required for migration, such as ICD-1 and CEH-22, do not regulate AC invasion (Cram et al., 2006; Lam et al., 2006; Matus et al., 2010). Examination of the similarities and differences in gene expression in the AC and DTCs may reveal modules specific for invasion or migration. For example, neither *zmp-1* or *cdh-3* are expressed in the DTCs, suggesting a specificity for cell invasion, and *mig-6* mutant alleles that cause severe DTC migration defects (Kawano et al., 2009) have only minor defects in invasion, suggesting a greater requirement for *mig-6* in migration.

HLH-2 regulates AC cytoskeletal polarity

Previous studies have shown that AC polarity is established by the coordinated action of the PAT-3/INA-1 integrin receptor complex and the UNC-6 (netrin) pathway (Hagedorn et al., 2009; Ziel et al., 2009). This work identifies a third pathway of polarization that enhances invasion defects in integrin and netrin mutant backgrounds. Reduction of HLH-2 function does not cause as severe a loss of polarity as seen in integrin or netrin mutants (Hagedorn et al., 2009; Ziel et al., 2009). Instead, the AC partially polarizes in *hlh-2* $L2_M$ RNAi-treated animals and *hlh-2(tm1768)* animals, but ectopic patches concentrate on the lateral and apical sides. The nature of this defect is unclear, but given HLH-2 regulation of BM components, could be due to impaired AC–BM interactions.

HLH-2 and the reiterative use of a transcription factor during specification and differentiation

HLH-2 has multiple roles in the AC prior to and during invasion. It first functions to endow Z1.ppp and Z4.aaa with the potential to become ACs. Later it functions to promote VU fate during the AC/VU decision (Karp and Greenwald, 2003, 2004). After the AC/VU decision, it regulates AC invasion (shown here). The downstream targets of HLH-2 during these processes appear to be distinct. The target(s) of HLH-2 that induce pro-AC competency are unknown. A target of HLH-2 during the AC/VU decision is *lag-2*, which is required for lateral LIN-

Please cite this article as: Schindler, A.J., Sherwood, D.R., The transcription factor HLH-2/E/Daughterless regulates anchor cell invasion across basement membrane in *C. elegans*, Dev. Biol. (2011), doi:10.1016/j.ydbio.2011.07.012

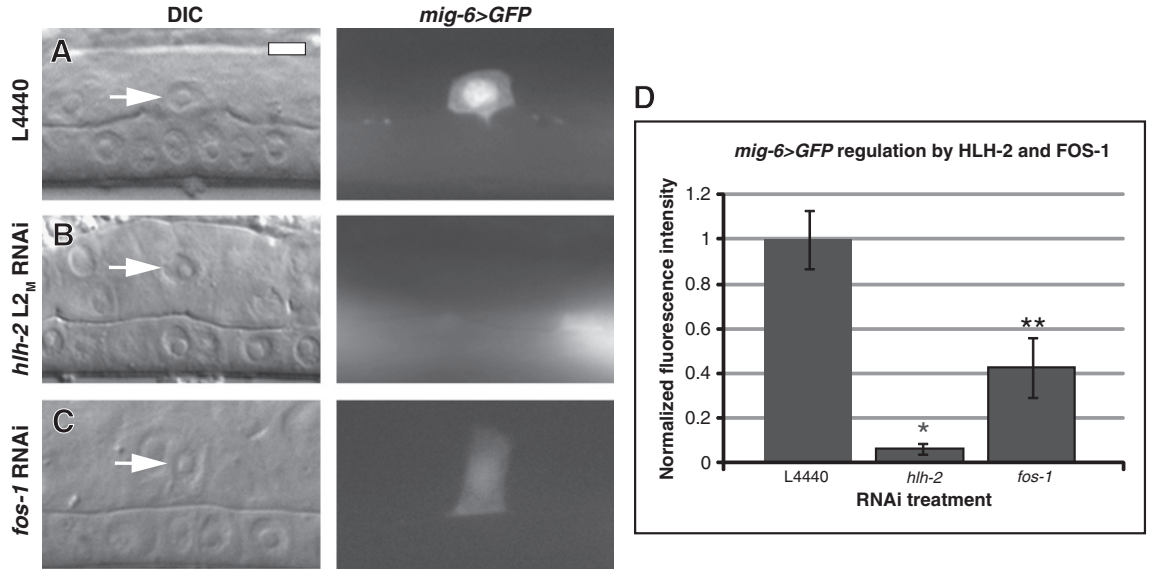

Fig. 6. *mig-6* is transcriptionally regulated by HLH-2 and FOS-1 in the AC. DIC images (left in each lettered pair) and corresponding *mig-6>GFP* fluorescence images (right in each lettered pair) at the mid-L3 stage. (A) L4440 control RNAi treatment with the AC expressing *mig-6>GFP* at the P6.p four-cell stage. (B) *hlh-2* $L2_M$ RNAi treatment results in undetectable *mig-6>GFP* expression, and (C) *fos-1* RNAi treatment reduces *mig-6>GFP* expression. (D) Quantification of RNAi treatment. *mig-6>GFP* expression is reduced 94% by *hlh-2* $L2_M$ RNAi treatment and 57% by *fos-1* RNAi treatment compared to control conditions. $n = 15$; $^{*}p < 1 \times 10^{-8}$; $^{**}p < .01$; error ± S.E.M.

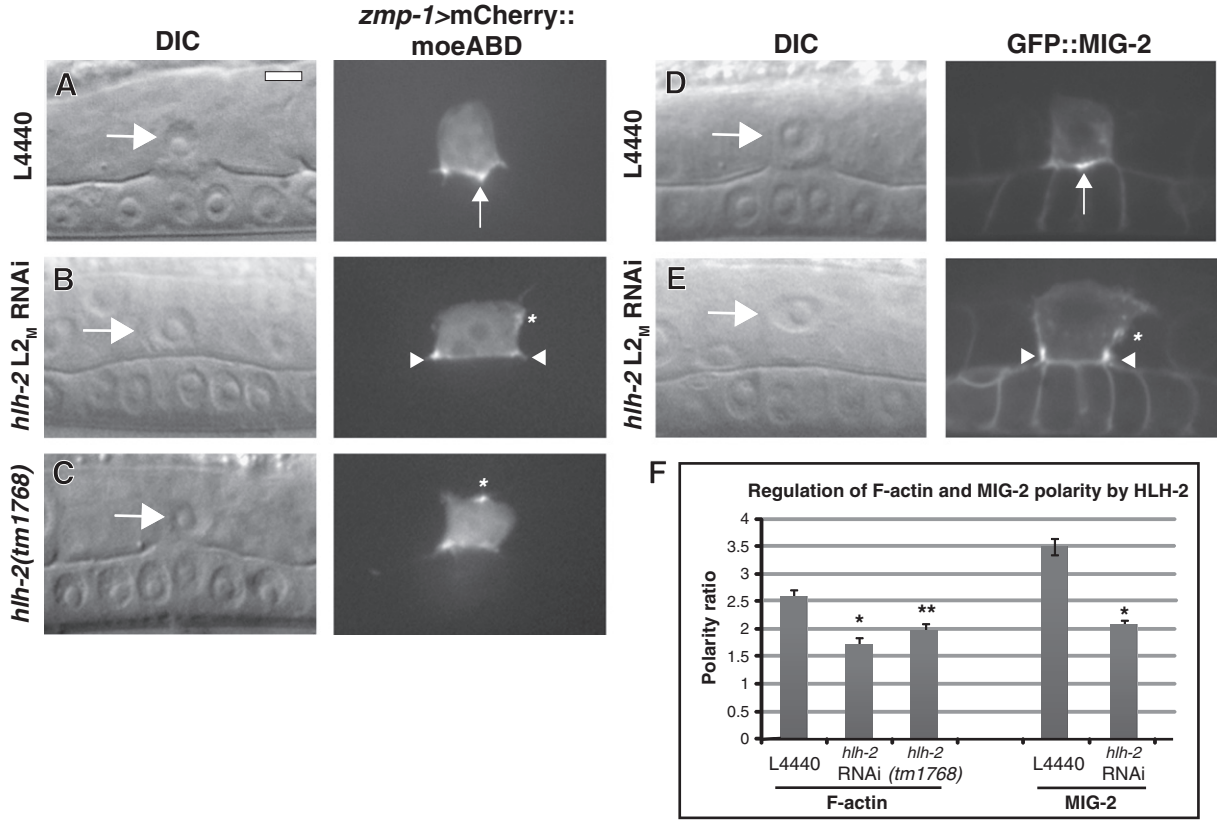

Fig. 7. HLH-2 is required for formation of the invasive cell membrane in the AC. (A–C) DIC images (left in each lettered pair) and corresponding fluorescence images (right in each lettered pair) at the mid-L3 stage of animals expressing the AC-specific F-actin binding protein *zmp-1*>mCherry::moesinABD. (A) In control L4440 RNAi treatment, F-actin localizes to the invasive membrane in contact with the BM and concentrates in the center of the AC between the two central 1° VPCs (arrow). (B) In *hlh-2* $L2_M$ RNAi-treated animals, AC invasion is blocked and F-actin localizes on the periphery of the ventral surface, away from the central 1° VPCs (arrowheads). An ectopic patch is mispolarized on the lateral side (asterisk). (C) Despite normal AC invasion in an *hlh-2(tm1768)* animal, an apical patch of F-actin is present on the AC plasma membrane (asterisk). (D–E) DIC images (left) and corresponding fluorescence images (right) in the mid-L3 stage of animals expressing the Rac GTPase GFP::MIG-2. (D) In control L4440 RNAi, GFP::MIG-2 concentrates on the ventral surface between the two central 1° VPCs (arrowhead). (E) In *hlh-2* $L2_M$ RNAi-treated animals, GFP::MIG-2 localizes on the periphery (arrowheads), and an ectopic patch is present on the lateral side (asterisk). (F) Quantification of F-actin and MIG-2 polarity in control (L4440) and *hlh-2* reduction-of-function conditions. Polarity ratio reflects the amount of mCherry::moesinABD or GFP::MIG-2 at the ventral invasive cell membrane relative to the apical and lateral surfaces. $n = 15$; $^{*}p < 1 \times 10^{-8}$; $^{**}p < 1 \times 10^{-3}$; error ± S.E.M.

Please cite this article as: Schindler, A.J., Sherwood, D.R., The transcription factor HLH-2/E/Daughterless regulates anchor cell invasion across basement membrane in *C. elegans*, Dev. Biol. (2011), doi:10.1016/j.ydbio.2011.07.012

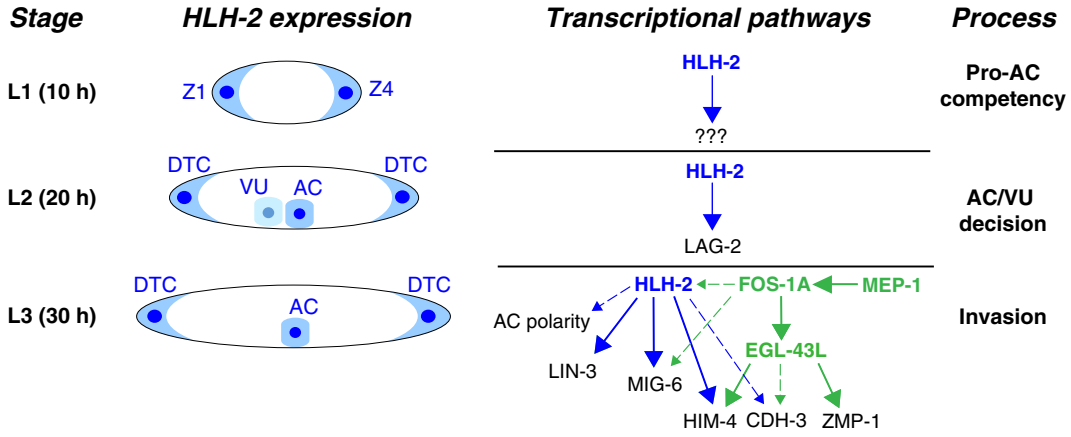

Fig. 8. Schematic diagram of HLH-2 expression and activity in the AC through the time of invasion. Time is post-hatch in hours at 20 °C. HLH-2 protein (blue) is expressed in the Z1/Z4 somatic gonadal precursor cells in the L1 stage, where it functions through unknown targets to regulate the competency of the Z1/Z4 descendants to adopt the AC lineage. In the L2 stage, HLH-2 is expressed in the AC and VU cells, and regulates *lag-2* transcription to suppress AC fate in the VU cell. Following the AC/VU decision, HLH-2 is reduced in the VU while remaining elevated in the AC (Karp and Greenwald, 2003). In the L3 stage, HLH-2 is expressed in the AC and regulates invasion. HLH-2 regulation of AC-expressed genes both overlaps and is independent from the FOS-1A transcriptional pathway. HLH-2 regulation is shown in blue; FOS-1A regulation is in green. Strong regulation is indicated with an unbroken arrow, and weaker regulation by a dashed arrow. HLH-2 and FOS-1A regulate *cdh-3* and *him-4* at similar levels (Sherwood et al., 2005), but HLH-2 regulates *mig-6* to a higher degree. HLH-2 independently regulates *lin-3* expression and cytoskeletal polarity, whereas FOS-1A independently regulates *egl-43L* and *zmp-1*. MEP-1 strongly regulates expression of FOS-1A protein (Matus et al., 2010), and FOS-1A partially regulates expression of HLH-2 protein.

12/Notch signaling (Karp and Greenwald, 2003). During invasion, HLH-2 regulates expression of *mig-6*, *him-4*, and *cdh-3*, all of which initiate expression after the AC/VU decision. Thus, HLH-2 is deployed at various developmental times within the same cell to regulate different genes and distinct biological processes. The ability to use staged RNAi treatments and the availability of weak alleles of *hlh-2* have helped to reveal the multiple roles of *hlh-2* in the AC lineage. This reiterative use of a transcription factor within a cell might be a prominent feature in *C. elegans*, where there has been a dramatic reduction in cell number and a concomitant increase of functions within each cell (Sternberg, 2001). As examples of this, the nuclear hormone receptor NHR-67/Tailless is required for both fate commitment and left/right patterning of chemosensory neurons (Sarin et al., 2009), and the bHLH transcription factor LIN-32/Atonal, acting with HLH-2, regulates specification, differentiation, and function of male ray sensory neurons (Portman and Emmons, 2000). Notably, however, multiple uses of transcription factors have also been documented in sea urchin primary mesenchyme cells (PMCs), in which the transcription factors twist and foxN2/3 control ingression and later aspects of PMC morphogenetic behaviors (Rho and McClay, 2011; Wu et al., 2008). Thus, the reiterative use of a transcription factor may be a common mechanism across phyla to link specification with the differentiated state of a cell.

Acknowledgments

We are grateful to J. Kimble for *hlh-2(tm1768)* and the *Caenorhabditis* Genetics Center for additional strains, and to E. Hagedorn, D. Matus, M. Morrissey, and J. Ziel for comments on the manuscript. This work was funded by a Pew Scholar's Award, a March of Dimes Basil O' Connor Award, and NIH Grant GM079320 to D.R.S. Author contributions: A.J.S. and D.R.S. designed experiments; A.J.S. and D.R.S. performed data acquisition and analysis; A.J.S and D.R.S. wrote and revised the manuscript.

Appendix A. Supplementary data

Supplementary data to this article can be found online at doi:10.1016/j.ydbio.2011.07.012.

References

Adiseshaiah, P., Vaz, M., Machireddy, N., Kalvakolanu, D.V., Reddy, S.P., 2008. A Fra-1-dependent, matrix metalloproteinase driven EGFR activation promotes human lung epithelial cell motility and invasion. J. Cell. Physiol. 216, 405–412.
Arnone, M.I., Davidson, E.H., 1997. The hardwiring of development: organization and function of genomic regulatory systems. Development 124, 1851–1864.
Brenner, S., 1974. The genetics of *Caenorhabditis elegans*. Genetics 77, 71–94.
Chesney, M.A., Lam, N., Morgan, D.E., Phillips, B.T., Kimble, J., 2009. *C. elegans* HLH-2/E/Daughterless controls key regulatory cells during gonadogenesis. Dev. Biol. 331, 14–25.
Cram, E.J., Shang, H., Schwarzbauer, J.E., 2006. A systematic RNA interference screen reveals a cell migration gene network in *C. elegans*. J. Cell Sci. 119, 4811–4818.
Gertler, F., Condeelis, J., 2011. Metastasis: tumor cells becoming MENAcing. Trends Cell Biol. 21, 81–90.
Hagedorn, E.J., Yashiro, H., Ziel, J.W., Ihara, S., Wang, Z., Sherwood, D.R., 2009. Integrin acts upstream of netrin signaling to regulate formation of the anchor cell's invasive membrane in *C. elegans*. Dev. Cell 17, 187–198.
Hedgecock, E.M., Culotti, J.G., Hall, D.H., 1990. The unc-5, unc-6, and unc-40 genes guide circumferential migrations of pioneer axons and mesodermal cells on the epidermis in *C. elegans*. Neuron 4, 61–85.
Hobert, O., 2002. PCR fusion-based approach to create reporter gene constructs for expression analysis in transgenic *C. elegans*. Biotechniques 32, 728–730.
Hwang, B.J., Sternberg, P.W., 2004. A cell-specific enhancer that specifies lin-3 expression in the *C. elegans* anchor cell for vulval development. Development 131, 143–151.
Hwang, B.J., Meruelo, A.D., Sternberg, P.W., 2007. *C. elegans* EVI1 proto-oncogene, EGL-43, is necessary for Notch-mediated cell fate specification and regulates cell invasion. Development 134, 669–679.
Ihara, S., Hagedorn, E.J., Morrissey, M.A., Chi, Q., Motegi, F., Kramer, J.M., Sherwood, D.R., 2011. Basement membrane sliding and targeted adhesion remodels tissue boundaries during uterine-vulval attachment in *Caenorhabditis elegans*. Nat. Cell Biol. 13, 641–651.
Inoue, T., Wang, M., Ririe, T.O., Fernandes, J.S., Sternberg, P.W., 2005. Transcriptional network underlying *Caenorhabditis elegans* vulval development. Proc. Natl. Acad. Sci. U. S. A. 102, 4972–4977.
Kao, G., Huang, C.C., Hedgecock, E.M., Hall, D.H., Wadsworth, W.G., 2006. The role of the laminin beta subunit in laminin heterotrimer assembly and basement membrane function and development in *C. elegans*. Dev. Biol. 290, 211–219.
Karp, X., Greenwald, I., 2003. Post-transcriptional regulation of the E/Daughterless ortholog HLH-2, negative feedback, and birth order bias during the AC/VU decision in *C. elegans*. Genes Dev. 17, 3100–3111.
Karp, X., Greenwald, I., 2004. Multiple roles for the E/Daughterless ortholog HLH-2 during *C. elegans* gonadogenesis. Dev. Biol. 272, 460–469.
Kawano, T., Zheng, H., Merz, D.C., Kohara, Y., Tamai, K.K., Nishiwaki, K., Culotti, J.G., 2009. *C. elegans* mig-6 encodes papilin isoforms that affect distinct aspects of DTC migration, and interacts genetically with mig-17 and collagen IV. Development 136, 1433–1442.
Kee, B.L., 2009. E and ID proteins branch out. Nat. Rev. Immunol. 9, 175–184.
Kirouac, M., Sternberg, P.W., 2003. cis-Regulatory control of three cell fate-specific genes in vulval organogenesis of *Caenorhabditis elegans* and *C. briggsae*. Dev. Biol. 257, 85–103.
Kustikova, O., Kramerov, D., Grigorian, M., Berezin, V., Bock, E., Lukanidin, E., Tulchinsky, E., 1998. Fra-1 induces morphological transformation and increases in vitro

invasiveness and motility of epithelioid adenocarcinoma cells. Mol. Cell. Biol. 18, 7095–7105.
Lam, N., Chesney, M.A., Kimble, J., 2006. Wnt signaling and CEH-22/tinman/Nkx2.5 specify a stem cell niche in *C. elegans*. Curr. Biol. 16, 287–295.
Lee, M., Cram, E.J., Shen, B., Schwarzbauer, J.E., 2001. Roles for beta(pat-3) integrins in development and function of *Caenorhabditis elegans* muscles and gonads. J. Biol. Chem. 276, 36404–36410.
Lifanov, A.P., Makeev, V.J., Nazina, A.G., Papatsenko, D.A., 2003. Homotypic regulatory clusters in *Drosophila*. Genome Res. 13, 579–588.
Luo, Y.P., Zhou, H., Krueger, J., Kaplan, C., Liao, D., Markowitz, D., Liu, C., Chen, T., Chuang, T.H., Xiang, R., Reisfeld, R.A., 2010. The role of proto-oncogene Fra-1 in remodeling the tumor microenvironment in support of breast tumor cell invasion and progression. Oncogene 29, 662–673.
Madsen, C.D., Sahai, E., 2010. Cancer dissemination—lessons from leukocytes. Dev. Cell 19, 13–26.
Matus, D.Q., Li, X.Y., Durbin, S., Agarwal, D., Chi, Q., Weiss, S.J., Sherwood, D.R., 2010. In vivo identification of regulators of cell invasion across basement membranes. Sci. Signal. 3, ra35.
Naito, Y., Yamada, T., Matsumiya, T., Ui-Tei, K., Saigo, K., Morishita, S., 2005. dsCheck: highly sensitive off-target search software for double-stranded RNA-mediated RNA interference. Nucleic Acids Res. 33, W589–W591.
Oliveri, P., Tu, Q., Davidson, E.H., 2008. Global regulatory logic for specification of an embryonic cell lineage. Proc. Natl. Acad. Sci. U. S. A. 105, 5955–5962.
Ozanne, B.W., Spence, H.J., McGarry, L.C., Hennigan, R.F., 2007. Transcription factors control invasion: AP-1 the first among equals. Oncogene 26, 1–10.
Perez-Moreno, M.A., Locascio, A., Rodrigo, I., Dhondt, G., Portillo, F., Nieto, M.A., Cano, A., 2001. A new role for E12/E47 in the repression of E-cadherin expression and epithelial–mesenchymal transitions. J. Biol. Chem. 276, 27424–27431.
Pollheimer, J., Knofler, M., 2005. Signalling pathways regulating the invasive differentiation of human trophoblasts: a review. Placenta 26 (Suppl. A), S21–30.
Portman, D.S., Emmons, S.W., 2000. The basic helix-loop-helix transcription factors LIN-32 and HLH-2 function together in multiple steps of a *C. elegans* neuronal sublineage. Development 127, 5415–5426.
Ramaswamy, S., Ross, K.N., Lander, E.S., Golub, T.R., 2003. A molecular signature of metastasis in primary solid tumors. Nat. Genet. 33, 49–54.
Rho, H.K., McClay, D.R., 2011. The control of foxN2/3 expression in sea urchin embryos and its function in the skeletogenic gene regulatory network. Development 138, 937–945.
Rimann, I., Hajnal, A., 2007. Regulation of anchor cell invasion and uterine cell fates by the egl-43 Evi-1 proto-oncogene in *Caenorhabditis elegans*. Dev. Biol. 308, 187–195.
Ririe, T.O., Fernandes, J.S., Sternberg, P.W., 2008. The *Caenorhabditis elegans* vulva: a post-embryonic gene regulatory network controlling organogenesis. Proc. Natl. Acad. Sci. U. S. A. 105, 20095–20099.
Rowe, R.G., Weiss, S.J., 2008. Breaching the basement membrane: who, when and how? Trends Cell Biol. 18, 560–574.
Rowe, R.G., Weiss, S.J., 2009. Navigating ECM barriers at the invasive front: the cancer cell-stroma interface. Annu. Rev. Cell Dev. Biol. 25, 567–595.
Sarin, S., Antonio, C., Tursun, B., Hobert, O., 2009. The *C. elegans* tailless/TLX transcription factor nhr-67 controls neuronal identity and left/right asymmetric fate diversification. Development 136, 2933–2944.
Sherwood, D.R., Sternberg, P.W., 2003. Anchor cell invasion into the vulval epithelium in *C. elegans*. Dev. Cell 5, 21–31.
Sherwood, D.R., Butler, J.A., Kramer, J.M., Sternberg, P.W., 2005. FOS-1 promotes basement-membrane removal during anchor-cell invasion in *C. elegans*. Cell 121, 951–962.
Slattery, C., McMorrow, T., Ryan, M.P., 2006. Overexpression of E2A proteins induces epithelial–mesenchymal transition in human renal proximal tubular epithelial cells suggesting a potential role in renal fibrosis. FEBS Lett. 580, 4021–4030.
Sobrado, V.R., Moreno-Bueno, G., Cubillo, E., Holt, L.J., Nieto, M.A., Portillo, F., Cano, A., 2009. The class I bHLH factors E2-2A and E2-2B regulate EMT. J. Cell Sci. 122, 1014–1024.
Sternberg, P.W., 2001. Working in the post-genomic *C. elegans* world. Cell 105, 173–176.
Tabara, H., Sarkissian, M., Kelly, W.G., Fleenor, J., Grishok, A., Timmons, L., Fire, A., Mello, C.C., 1999. The rde-1 gene, RNA interference, and transposon silencing in *C. elegans*. Cell 99, 123–132.
Tamai, K.K., Nishiwaki, K., 2007. bHLH transcription factors regulate organ morphogenesis via activation of an ADAMTS protease in *C. elegans*. Dev. Biol. 308, 562–571.
Thiery, J.P., Acloque, H., Huang, R.Y., Nieto, M.A., 2009. Epithelial–mesenchymal transitions in development and disease. Cell 139, 871–890.
Uhlirova, M., Bohmann, D., 2006. JNK- and Fos-regulated Mmp1 expression cooperates with Ras to induce invasive tumors in *Drosophila*. EMBO J. 25, 5294–5304.
van 't Veer, L.J., Dai, H., van de Vijver, M.J., He, Y.D., Hart, A.A., Mao, M., Peterse, H.L., van der Kooy, K., Marton, M.J., Witteveen, A.T., Schreiber, G.J., Kerkhoven, R.M., Roberts, C., Linsley, P.S., Bernards, R., Friend, S.H., 2002. Gene expression profiling predicts clinical outcome of breast cancer. Nature 415, 530–536.
Vogel, B.E., Hedgecock, E.M., 2001. Hemicentin, a conserved extracellular member of the immunoglobulin superfamily, organizes epithelial and other cell attachments into oriented line-shaped junctions. Development 128, 883–894.
Wang, W., Wyckoff, J.B., Frohlich, V.C., Oleynikov, Y., Huttelmaier, S., Zavadil, J., Cermak, L., Bottinger, E.P., Singer, R.H., White, J.G., Segall, J.E., Condeelis, J.S., 2002. Single cell behavior in metastatic primary mammary tumors correlated with gene expression patterns revealed by molecular profiling. Cancer Res. 62, 6278–6288.
Wang, W., Goswami, S., Sahai, E., Wyckoff, J.B., Segall, J.E., Condeelis, J.S., 2005. Tumor cells caught in the act of invading: their strategy for enhanced cell motility. Trends Cell Biol. 15, 138–145.
Wilkinson, H.A., Fitzgerald, K., Greenwald, I., 1994. Reciprocal changes in expression of the receptor lin-12 and its ligand lag-2 prior to commitment in a *C. elegans* cell fate decision. Cell 79, 1187–1198.
Wu, S.Y., Yang, Y.P., McClay, D.R., 2008. Twist is an essential regulator of the skeletogenic gene regulatory network in the sea urchin embryo. Dev. Biol. 319, 406–415.
Yilmaz, M., Christofori, G., 2009. EMT, the cytoskeleton, and cancer cell invasion. Cancer Metastasis Rev. 28, 15–33.
Ziel, J.W., Hagedorn, E.J., Audhya, A., Sherwood, D.R., 2009. UNC-6 (netrin) orients the invasive membrane of the anchor cell in *C. elegans*. Nat. Cell Biol. 11, 183–189.

Please cite this article as: Schindler, A.J., Sherwood, D.R., The transcription factor HLH-2/E/Daughterless regulates anchor cell invasion across basement membrane in *C. elegans*, Dev. Biol. (2011), doi:10.1016/j.ydbio.2011.07.012